Spatial patterns in the oxygen isotope composition of daily rainfall in the British Isles

Jonathan Tyler[1,2*]
Matthew Jones[3,6]
Carol Arrowsmith[4]
Tim Allott[5]
Melanie J. Leng[4,6]

1 Department of Earth Sciences, The University of Adelaide, Adelaide, South Australia, 5005, Australia.
2 Sprigg Geobiology Centre, The University of Adelaide, Adelaide, South Australia, 5005, Australia.
3 School of Geography, The University of Nottingham, University Park, Nottingham, NG7 2RD, United Kingdom.
4 NERC Isotope Geosciences Facilities, British Geological Survey, Keyworth, Nottingham, NG12 5GG, United Kingdom.
5 Met Office, FitzRoy Road, Exeter, Devon, EX1 3PB, United Kingdom.
6 Centre for Environmental Geochemistry, The University of Nottingham, University Park, Nottingham, NG7 2RD, United Kingdom.

* Corresponding author: jonathan.tyler@adelaide.edu.au

Abstract

Understanding the modern day relationship between climate and the oxygen isotopic composition of precipitation ($\delta^{18}O_P$) is crucial for obtaining rigorous palaeoclimate reconstructions from a variety of archives. To date, the majority of empirical studies into the meteorological controls over $\delta^{18}O_P$ rely upon daily, event scale, or monthly time series from individual locations, resulting in uncertainties concerning the representativeness of statistical models and the mechanisms behind those relationships. Here, we take an alternative approach by analysing daily patterns in $\delta^{18}O_P$ from multiple stations across the British Isles (n = 10 - 70 stations). We use these data to examine the spatial and seasonal heterogeneity of regression statistics between $\delta^{18}O_P$ and common predictors (temperature, precipitation amount and the North Atlantic Oscillation index; NAO). Temperature and NAO are poor predictors of daily $\delta^{18}O_P$ in the British Isles, exhibiting weak and/or inconsistent effects both spatially and between seasons. By contrast $\delta^{18}O_P$ and rainfall amount consistently correlate at most locations, and for all months analysed, with spatial and temporal variability in the regression coefficients. The maps also allow comparison with daily synoptic weather types, and suggest characteristic $\delta^{18}O_P$ patterns, particularly associated with Cylonic Lamb Weather Types. Mapping daily $\delta^{18}O_P$ across the British Isles therefore provides a more coherent picture of the patterns in $\delta^{18}O_P$, which will ultimately lead to a better understanding of the climatic controls. These observations are another step forward towards developing a more detailed, mechanistic framework for interpreting stable isotopes in rainfall as a palaeoclimate and hydrological tracer.

Keywords: oxygen isotopes, amount effect, NAO, British Isles

Introduction

The relationship between climate and the oxygen isotope composition of precipitation ($\delta^{18}O_P$) is central to a wide range of palaeoclimate interpretation techniques, from direct archives of ancient precipitation preserved in ice (e.g. Barbante et al. 2006; Dansgaard et al. 1993; Johnsen et al. 2001; Petit et al. 1999), through indirect archives which include speleothem calcite, lake sediment biominerals and tree ring cellulose (e.g. Baker et al. 2011; Evans and Schrag 2004; Jones et al. 2006; Robertson et al. 2001; Tyler et al. 2008; von Grafenstein et al. 1996; Wang et al. 2008). Improved understanding of the climate-isotope relationship is therefore an important step towards improving the accuracy and rigour of palaeoclimate reconstructions both from individual records and through regional/global data-assimilation projects (e.g. PAGES 2k Consortium 2013; Shakun and Carlson 2010). Much of our understanding of this key climate-isotope interaction is built around two approaches: the development and exploration of isotope-enabled climate models (Gedzelman and Arnold 1994; Hoffmann et al. 2006; Jouzel et al. 2000; Langebroek et al. 2011; Merlivat and Jouzel 1979; Schmidt et al. 2007) and the statistical examination of isotope monitoring data (Dansgaard 1964; Fischer and Baldini 2011; Rozanski et al. 1993; Treble et al. 2005). Despite significant developments in incorporating isotope systematics into climate models, the continued acquisition and exploration of precipitation isotope monitoring data remains crucial, both to assist in the validation and parameterisation of climate models but also to refine the interpretation of isotope based palaeoclimate records.

Empirical studies into the links between $\delta^{18}O_P$ and climatic/meteorological parameters are numerous and diverse. A widespread correlation between $\delta^{18}O_P$ and air temperature is manifest globally and for select continental regions, particularly from a spatial perspective and occasionally through time (Araguas-Araguas et al. 2000; Dansgaard 1964; Kohn and Welker 2005; Rozanski et al. 1993). Air temperature is an important factor in driving condensation within a vapour parcel and dictating the liquid-vapour isotopic fractionation (Dansgaard 1964). However, uncertainties exist regarding the association between air temperature at the land surface and vapour condensation temperature, which varies as a function of altitude even during the course of an individual rainfall event (Celle-Jeanton et al. 2004; Celle-Jeanton et al. 2001). Furthermore, the global correlation between air temperature and $\delta^{18}O_P$ is subject to covariance with other key elements of the global isotope hydrological cycle, including latitude, conditions at and distance from evaporation source, and precipitation amount (Bowen and Wilkinson 2002).

Changes in precipitation amount are also expected to impart an influence upon $\delta^{18}O_P$, due to the combined effects of Rayleigh distillation prior to precipitation at the monitoring station, evaporation from falling raindrops and isotopic exchange between raindrops and ambient vapour beneath cloud level (Callow et al. 2014; Dansgaard 1964). The so called 'amount effect' is most prominently associated with convective tropical rainfall (Rozanski et al. 1993), however correlations between rainfall amount and $\delta^{18}O_P$ have also been frequently observed in data from maritime temperate regions (Baldini et al. 2010; Baldini et al. 2008; Callow et al. 2014; Celle-Jeanton et al. 2001; Crawford et al. 2013; Darling and Talbot 2003; Treble et al. 2005). In addition to effects at the site of precipitation, variability in $\delta^{18}O_P$ is subject to the

100 conditions at the source of moisture evaporation (e.g. sea surface temperatures and
101 relative humidity), the trajectory of the air mass, synoptic weather patterns and
102 interaction with the land surface (Celle-Jeanton et al. 2004; Celle-Jeanton et al. 2001;
103 Fischer and Baldini 2011; Heathcote and Lloyd 1986; Lachniet and Patterson 2009;
104 Liebminger et al. 2006; Sodemann et al. 2008; Treble et al. 2005).
105
106 A major advance in our understanding of the controls over $\delta^{18}O_P$ has been the
107 proliferation of studies utilising daily or event-scale monitoring in an attempt to
108 address the mechanisms behind isotopic signatures at timescales relevant to the actual
109 process (Baldini et al. 2010; Fischer and Baldini 2011; Heathcote and Lloyd 1986).
110 Longer term $\delta^{18}O_P$ data – be they monthly, annual, centennial or millennial – are best
111 viewed as composites of event scale processes, weighted by the amount of rainfall
112 during each event. For this reason, regression models built around monthly or annual
113 data can be subject to issues related to changes in seasonal weighting (Vachon et al.
114 2007) or simply an inability to capture the conditions during which precipitation
115 occurred (Baldini et al. 2010). Recently, approaches have emerged which enable the
116 integration of monthly resolved isotope data with daily meteorological data, therefore
117 modelling the processes at timescales relevant to synoptic conditions (Fischer and
118 Baldini 2011; Fischer and Treble 2008). However, with increased resolution comes
119 increased noise, thus the representativeness of empirical models based upon single
120 isotope time-series comes into question. There is therefore significant value in studies
121 which combine daily monitoring with multiple sites in order to evaluate the
122 relationships between regional meteorology and the isotopic composition of
123 precipitation (e.g. Good et al. 2014) and such studies are scarce.
124

125 The British Isles is an interesting study location for isotopes in rainfall, with a
126 maritime climate that is affected by the confluence of weather systems with distinctly
127 different origins depending on the direction of flow (Heathcote and Lloyd 1986).
128 Previous studies have addressed the climate-isotope relationships in the British Isles
129 using single site daily, event based and monthly monitoring (Baldini et al. 2010;
130 Darling and Talbot 2003; Fischer and Baldini 2011; Heathcote and Lloyd 1986; Jones
131 et al. 2007). On the basis of nearly two year's daily monitoring at Driby, Lincolnshire,
132 Heathcote and Lloyd (1986) observed no correlation between air temperature and
133 $\delta^{18}O_P$ and concluded that weather type and associated origin of moisture is the
134 primary factor responsible for changes in daily $\delta^{18}O_P$. At Wallingford, Oxfordshire,
135 Darling and Talbot (2003) observed weak and seasonally variable correlations
136 between daily $\delta^{18}O_P$, temperature and precipitation amount – correlations which
137 improve when monthly values are used. In a detailed analysis of event scale $\delta^{18}O_P$ in
138 Dublin, Ireland, Baldini et al. (2008; 2010) demonstrate the primary role of
139 precipitation amount and moisture source trajectory. On the basis of those data,
140 Fischer and Baldini (2011), developed a series of daily empirical functions of
141 increasing complexity to characterise $\delta^{18}O_P$ as a function of precipitation amount and
142 moisture source. The Fischer and Baldini (2011) daily functions, and approach in
143 general, offer tremendous potential for improving the interpretation of palaeoclimate
144 archives. However, the broader applicability of those functions, as with the traditional
145 Dansgaard (1964) type relationships, is dependent upon understanding how the
146 coefficients and model skill vary in space and through time. In particular, the causal
147 mechanism between rainfall amount and $\delta^{18}O_P$, and how that relationship evolves
148 through the lifespan of a rainfall event, remains poorly understood. Here, in an
149 attempt to better evaluate the spatial and temporal heterogeneity of daily isotope

functions, and to address the issue of signal vs. noise in daily $\delta^{18}O_P$ data, daily monitoring of $\delta^{18}O_P$ was carried out at multiple locations across the relatively small spatial gradient of the British Isles. We report daily $\delta^{18}O$ measurements over 57 days, sampling rainfall events across each of the four seasons from up to 70 sites. These data indicate daily spatial $\delta^{18}O$ gradients within the British Isles of up to 17‰, highlighting the role of the evolution of weather systems in driving local scale variability in $\delta^{18}O_P$. We use these data to evaluate the empirical relationships between $\delta^{18}O_P$ and daily weather, and to qualitatively assess the potential for developing a synoptic typology for $\delta^{18}O_P$ in the British Isles.

Sites and Methodology

Daily precipitation water samples were collected from up to 70 sites within England, Wales, Scotland and Northern Ireland (Figure 1; Table 1). The samples were collected as part of a pilot study for the British Isotopes in Rainfall Project (BIRP) - a community engagement initiative, in collaboration with volunteer weather observers and the UK Met Office. Initially, 17 volunteers were engaged, contacted via the Climate Observers Link (COL) or via existing monitoring programmes (Table 1). This group was subsequently augmented by further weather observers with ongoing association with the U.K. Met Office. Precipitation water samples were collected using a standard Met Office rain gauge at 9 am GMT each day. Having measured the amount of rainfall for the previous 24 hours, the rain water samples were transferred to 4 ml or 8 ml Nalgene ® HDPE bottles, depending on rainfall amount taking care to ensure bottles were full to avoid any exchange of sample oxygen with air in the bottle. The bottles were labelled, stored at 4ºC and sent to the British Geological Survey at

175 the end of each month. Details of sampling practice were communicated to
176 participants via an online video (http://tinyurl.com/BIRP2010), with further
177 instructions provided via post to each sampler.
178
179 Precipitation samples were collected during the course of four campaigns, conducted
180 in March 2010, October 2010, July 2011 and January 2012, thereby capturing a
181 subsample of each of the seasons. Collection days were inevitably limited by the
182 occurrence of precipitation events and availability of volunteers, and thus the sample
183 set for each site and month range from 2-19 samples (Table 1). In addition to
184 collecting precipitation water, at the majority of stations a range of meteorological
185 data was recorded. Every station provided rainfall amount data, and the majority also
186 provided air temperature recordings. Where local temperature readings were not
187 taken, temperature data from a nearby Met Office station was used (Table 1). Because
188 precipitation samples were collected at 9 am each day, the date of precipitation in
189 each instance was assigned as the previous day, both for precipitation amount data
190 and isotope composition, following standard practice for the U.K. Met Office. The
191 daily North Atlantic Oscillation (NAO) index was obtained from the U.S. National
192 Oceanic and Atmospheric Administration (NOAA) Climate Prediction Center
193 (http://www.cpc.ncep.noaa.gov).
194
195 Oxygen and hydrogen isotopes of water were analysed at NERC Isotope Geosciences
196 Facility at the British Geological Survey. For D/H analysis, the hydrogen was
197 liberated by Cr reduction, while $^{18}O/^{16}O$ were equilibrated with CO_2 using an
198 ISOPREP 18 device. Mass spectrometry was performed on a VG SIRA ($\delta^{18}O$) and

IsoPrime (δ^2H) in conjunction with laboratory standards calibrated against NBS standards. Long term analytical errors are 0.05‰ for $\delta^{18}O$ and <1‰ for δ^2H.

Spatial patterns in daily $\delta^{18}O_P$ were mapped using the *filled.contour3()* program in R, which uses the function *akima()* to perform bivariate data interpolation (Akima 1978). Backward trajectories of air parcels arriving at the British Isles were computed using the web-based HYbrid Single-Particle Lagrangian Integrated Trajectory (HYSPLIT) model (Draxler and Hess 1997; Draxler and Hess 1998; Draxler and Rolph 2015; Rolph 2015) for a matrix of 63 locations between 5.7ºW, 50ºN and 2.7ºE, 58ºN. Back trajectories were computed for air parcels arriving at 1500 m.a.s.l. at six-hourly intervals prior to the time of water sampling at 9:00 hrs. Principle locations of moisture uptake were estimated as the first point in a particular trajectory whereby the specific humidity increased by >0.5 g/kg and atmospheric pressure was >900 hPa, following Krklec and Dominguez-Villar (2014).

Results

Regression between daily $\delta^{18}O_P$, maximum air temperature and precipitation amount

For the statistical analysis of daily precipitation isotope data, we treat the data from January 2012 separately from those from March 2010, October 2010 and July 2011. This is because the January 2012 sample contains observations from ~4 times as many locations, yet over three days, which contrasts with the fewer (15-17) locations over up to 19 days for the other sampling months. In all instances, relationships with precipitation amount are explored using a power coefficient ($P^{0.5}$), to ensure a

224 Gaussian distribution of regression residuals, following the reasoning outlined in
225 Fischer and Treble (2008) and Fischer and Baldini (2011); nonlinear relationships are
226 known in climate-isotope studies, such as in the discussion of Rayleigh fractionation
227 later in this paper, and root transformations are often applied to precipitation data in
228 climatology because precipitation data are typically skewed. Daily maximum
229 temperatures (T_{max}) are used, since they relate to the temperature around noon on the
230 day of precipitation, whereas mean daily temperatures for the period of sampling (9
231 am - 9 am) are not consistently available.

232

233 The relationship between $\delta^{18}O_P$, T_{max} and $P^{0.5}$ is explored first using all daily data
234 (excluding January 2012), and then with data subset according to month and site in
235 order to ascertain the consistency of relationships in time and space. Due to the
236 paucity of data, monthly subsets from each site were not analysed individually. When
237 all daily data are combined, there are weak yet statistically significant ($p < 0.001$)
238 relationships between $\delta^{18}O_P$, $P^{0.5}$ *and* T_{max} (r^2 = 0.17 and 0.02 respectively) but not
239 NAO (Figure 2). Significant regressions can also be observed between $\delta^{18}O_P$ and $P^{0.5}$
240 when data are subset according to month, with slope coefficients varying between
241 March 2010 (slope = –1.45, r^2 = 0.24), October 2010 (slope = –0.97, r^2 = 0.14) and
242 July 2011 (slope = –0.85, r^2 = 0.19) (Figure 3a-c). Significant regressions ($p < 0.05$)
243 did not exist between $\delta^{18}O_P$ and T_{max} for monthly subsets for March or October 2010
244 (Figure 3d-e), however a weak (r^2 = 0.04, p = 0.01) relationship was observed for July
245 2011 (Figure 3f). The mean T_{max} for the three sampled months varied markedly, from
246 10.54ºC in March 2010, 12.74ºC in October 2010 and 17.21ºC in July 2011 (Figure

247 3d-f). There were no significant regressions ($p < 0.05$) between $\delta^{18}O_P$ and NAO
248 where data were subset according to month (Figure 3g-i).
249
250 When data are subset according to sampling location (incorporating data from each
251 month excluding January 2012), significant regressions between $\delta^{18}O_P$ and $P^{0.5}$ can be
252 observed with $p < 0.05$ at 11 of the 17 sites (Figure 4). Those sites that did not exhibit
253 significant precipitation effects were Edenbridge (EDEN), Glenmore Lodge (GLEN),
254 Horsham (HOR), Lunan Valley (LUNA), Wallingford (WALL) and West Moors
255 (WMOR) (Figure 4). Five sites exhibited significant $P^{0.5}$ effects with $r^2 > 0.3$, and
256 those were Acton (ACT), Aboyne (ABYE), Carlton-in-Cleveland (CACL), Darvel
257 (DAR) and Lawkland (LAW). Given the paucity of data, it was not possible to
258 rigorously test for differences in the within-site $P^{0.5}$ vs. $\delta^{18}O_P$ relationships between
259 months, although there is no obvious indication that data from March 2010, October
260 2010 or July 2011 exhibit markedly different response patterns to the regression
261 models based on all months combined (Figure 4).
262
263 Five of the 17 site-specific regressions between T_{max} and $\delta^{18}O_P$ are significant to $p <$
264 0.05, data from Acton (ACT), Ebbr Vale (EBBV), Glenmore Lodge (GLEN),
265 Marlborough (MARL) and Wallingford (WALL) (Figure 5). The slope coefficients
266 for those relationships range between +0.14 at Glenmore Lodge (GLEN) to +0.37 at
267 Acton (ACT). For most sites, particularly those with significant T_{max} effects, there is
268 visible clustering of data according to month (Figure 5). There is only one site,
269 Edenbridge (EDEN) which exhibits a significant ($p < 0.05$, $r^2 = 0.58$) positive
270 relationship with NAO, however only a single month (March) was monitored at that
271 site (Figure 6). Two additional sites – West Moors (WMOR) and Horsham (HOR)

also exhibited significant regressions between March $\delta^{18}O_P$ and NAO (Supplementary Information, Figure S1).

The spatial distribution of regression coefficients for $P^{0.5}$ and T_{max} vs. $\delta^{18}O_P$ are mapped in Figure 7. Sites which exhibit significant regression coefficients between $\delta^{18}O_P$ and $P^{0.5}$ are distributed across the British Isles, however the sites with the largest r^2 and lowest (most negative) slopes vs. $P^{0.5}$ are those in northern England and Scotland, with the exception of Acton (ACT) in central England (Figures 7a and 7b). Two sites in Scotland, Glenmore Lodge (GLEN) and Lunan Valley (LUNA), exhibit no significant relationship with $P^{0.5}$ (Figures 7a and 7b). Only five sites produced a significant regression between $\delta^{18}O_P$ and T_{max}, of which four are situated in central and southern England (Figures 7c and 7d). One northern site – Glenmore Lodge (GLEN), Scotland, also exhibited a significant relationship with temperature, whilst three sites on the southern coast of England exhibited no significant temperature effect (Figures 7c and 7d).

Spatial distribution of daily $\delta^{18}O_P$

Over the sampling period, the geographical distribution of $\delta^{18}O_P$ across Great Britain varied markedly from day to day. On some occasions, e.g. 13th March 2010 (Figure S2), 17th October 2010 (Figure S3) and 21st July 2011 (Figure S4), $\delta^{18}O_P$ values were largely homogenous (within a 2‰ range) across the entire spatial gradient. However, on other occasions, e.g. 4th October 2010, 27th October 2010 (Figure S3) and 9th July 2011 (Figure S4), marked spatial gradients in $\delta^{18}O_P$ occurred, up to a maximum range of 17‰. The degree of spatial homogeneity may, in part, relate to the sampling

297 frequency and location of precipitation samples for a particular day, however the day
298 to day differences in spatial range measured from ~15 sites is equivalent to that
299 observed over the three days sampled in January 2012 (Figure 8), where the spatial
300 gradient varies from 17‰ on 23rd January 2012 to 10‰ on 25th January 2012, despite
301 over 60 stations being sampled on both occasions. Most frequently, daily $\delta^{18}O_P$
302 patterns show a decrease along a south-west to north-east gradient, although there are
303 numerous exceptions to this rule, with occasional inversions in the south-west to
304 north-east gradient, changes in the direction of that gradient and bimodal distributions
305 (e.g. 20th March 2010, 22nd October 2010 and 6th July 2011; Figures S2-S4). The most
306 depleted $\delta^{18}O_P$ values measured were collected at sites in Scotland and northern
307 England. Although a larger density of samples is preferable in order to trace spatial
308 patterns in daily $\delta^{18}O_P$, reduction in sample number to as few as four sites still allows
309 for some coherent patterns to be observed. On days where precipitation fell at all
310 locations, the pattern which emerges from 14 sampling sites (e.g. 17th July 2011,
311 Figure S4) is not dissimilar to those which can be observed based upon >80 sites (e.g.
312 24th January 2012; Figure 8c).
313
314 Spatial patterns in $\delta^{18}O_P$ are clearly best captured in January 2012, where the sample
315 density was highest (Figure 8). On 23rd January 2012, the lowest $\delta^{18}O_P$ values of –
316 18.5‰ were obtained from rain falling in eastern-central Scotland, with a pattern of
317 increasing $\delta^{18}O_P$ to the north, west and particularly to the south of that location
318 (Figure 8c). On this date, western England and Wales, Northern Ireland and southeast
319 England experienced the highest $\delta^{18}O_P$ values of upto 0.58‰, with a southward
320 pattern of increasing $\delta^{18}O_P$ along the eastern coast of England (Figure 8c). On 24th
321 January 2012, a marked longitudinal gradient was observed, with declining $\delta^{18}O_P$

322 along an east-northeast trajectory (Figure 8f). Lowest $\delta^{18}O_P$ values on 24th January
323 were observed along the eastern coast of England and Scotland (Figure 8f). The 25th
324 January 2012 saw a shift towards low $\delta^{18}O_P$ (–15 to –10‰) in the north west of
325 Scotland, Northern Ireland, north west England and northern Wales, with higher
326 $\delta^{18}O_P$ in the south of England (Figure 8i). HYSPLIT modelling indicates that two
327 moisture bearing air masses crossed the British Isles on January 23rd, 2012 (Figures 8a
328 and 8b). The first parcel collected water vapour over the Norwegian Sea, east of
329 Iceland and collided with the northern British Isles along a north-westerly trajectory
330 (Figure 8a). The second air mass collected moisture from the central Atlantic Ocean
331 and collided with the British Isles along a south-westerly trajectory. On the 24th
332 January 2012, HYSPLIT modelling indicates that the majority of moisture was
333 derived from the central Atlantic, impacting the British Isles along a westerly/south-
334 westerly trajectory (Figure 8d). On the 25th January 2012, HYSPLIT modelling
335 indicates moisture arriving from a south-westerly trajectory, having markedly
336 changed direction beforehand above the Bay of Biscay to the south (Figure 8g).
337
338 The relationship between the spatial distribution of $\delta^{18}O_P$ and synoptic weather types,
339 as classified through the Lamb Weather Type scheme (LWT; Jones et al. 1993; Lamb
340 1950) is explored in Figures 9 and 10. The majority of rainfall events during the
341 studied period were associated with two principle weather types: Cyclonic (LWT =
342 20) and South Westerly (LWT = 15) (Figure S5). Under the influence of Cyclonic
343 weather types, $\delta^{18}O_P$ exhibits a pattern of higher values in southern and south-west
344 England contrasting with a frequently occurring region of markedly lower $\delta^{18}O_P$ over
345 northern England and southern Scotland (Figure 9). Occasionally, those lower $\delta^{18}O_P$
346 values extend southwards along the eastern coast of England, e.g. on 8th July 2011 and

347 17th July 2011 (Figure 9). Higher $\delta^{18}O_P$ values can also be observed to the far north
348 during these weather events, e.g. on 3rd October 2010, 8th July 2011 and 18th July
349 2011 (Figure 9). Under the influence of South Westerly weather, a consistent spatial
350 pattern in $\delta^{18}O_P$ is not evident and many of these days exhibit a narrow range of $\delta^{18}O_P$
351 (<5‰). On the 24th January 2012, $\delta^{18}O_P$ values largely exhibit a SW-NE gradient
352 across Great Britain, except for low $\delta^{18}O_P$ at Llansadwryn (LLAN), North Wales
353 (Figure 10). By contrast, on 10th October 2010, the lowest $\delta^{18}O_P$ values were recorded
354 in the south west of England and Wales. On other days (e.g. 18th March 2010; 23rd
355 March 2010), the lowest or highest $\delta^{18}O_P$ values were recorded in northern-central
356 England.
357
358 **Discussion**
359
360 Daily monitoring of isotopes in rainfall, on the basis of 57 days and 17 sites, support
361 previous observations that square root transformed daily precipitation amount ($P^{0.5}$) is
362 the most consistent predictor of daily $\delta^{18}O_P$ in maritime, mid-latitude regions (Baldini
363 et al. 2010; Fischer and Baldini 2011; Fischer and Treble 2008). All data combined
364 (including January 2012) define a daily function $\delta^{18}O_{P\text{-}day} = (-0.9)P^{0.5}{}_{day} - 4.7$, $r^2 =$
365 0.1 (Figure 2a) which is very similar to the model derived by Baldini et al. (2010)
366 based on two years monitoring of event based $\delta^{18}O_P$ at Dublin, Ireland (Baldini et al.
367 2010; Fischer and Baldini 2011) and with the relationship between daily $\delta^{18}O_P$ and
368 $P^{0.5}$ at Wallingford, England, between November 1979-October 1980 (data reported
369 by Darling and Talbot 2003). The $P^{0.5}$ regression coefficients derived when data are
370 subset according to month (Figure 3) and by site (Figure 4) vary compared to those
371 based on the whole dataset combined. Firstly, the regression slope varies between the

three months studied, suggestive of a seasonally modulated relationship between $\delta^{18}O_P$ and $P^{0.5}$ as described by Fischer and Baldini (2011). Indeed, the $P^{0.5}$ coefficients obtained here (Figure 3) are consistent with those predicted by Equation 8 in Fischer and Baldini (2011) for March and October 2010 (–1.45 and –0.97 respectively) but not for July 2011, where our data indicate a slope of –0.85 compared to a predicted –0.41. Secondly, the $P^{0.5}$ coefficients vary spatially: steeper negative slope coefficients and higher r^2 values are generally observed in northern England and Scotland compared to larger slope coefficients and less frequent significant relationships at sites in southern England (Figure 7). One exception to this rule - Acton (ACT) - is located in the English west midlands in the rain shadow of the Welsh mountains (Figure 7a). We will discuss potential reasons for the variable $\delta^{18}O_P$–$P^{0.5}$ relationship at the end of this section.

The relationship between air temperature and daily $\delta^{18}O_P$ is less convincing. A weak yet significant correlation is observed between daily $\delta^{18}O_P$ and daily maximum air temperature (T_{max}) based on all samples (Figure 2b). At first glance, this apparent temperature effect appears to support previous observations, based on global compilations of monthly data (e.g. Araguas-Araguas et al. 2000; Dansgaard 1964; Rozanski et al. 1993; Rozanski et al. 1992). Furthermore, a temperature effect has some theoretical grounding, since changes in temperature affect the vapour-liquid fractionation factor during condensation (Dansgaard 1964; Merlivat 1978; Merlivat and Nief 1967). However the relationship between T_{max} and $\delta^{18}O_P$ does not consistently hold when samples are subset according to month or site, with only the July 2011 monthly subset and 5 out of 17 site-specific analyses producing a significant T_{max} regression (Figures 3, 5 and 7). In addition, as is the case with $P^{0.5}$, the

occurrence of significant relationships with T_{max} varies spatially, with predominantly southern and central sites exhibiting T_{max} effects (Figure 7c and d). One of those sites is Wallingford (WALL), for which Darling and Talbot (2003) observed significant positive correlations between daily average air temperature and daily $\delta^{18}O_P$ for winter (DJF) and autumn (OSN) precipitation (sampled between November 1979 - October 1980). The coefficients of those 1979-1980 models are similar to those derived for July 2011 (Figure 3f). However, Darling and Talbot (2003) did not observe a significant relationship with temperature during summer precipitation at Wallingford, further highlighting the inconsistency of temperature-based regression with daily $\delta^{18}O_P$. Three sites along the southern English coast exhibit no significant relationship between $\delta^{18}O_P$ and T_{max}, whilst another site, Glenmore Lodge in Scotland, does (Figures 7c and 7d). It is therefore not possible to make generalisations concerning the spatial patterns in T_{max} effects upon $\delta^{18}O_P$. One potential explanation for the correlation between T_{max} and $\delta^{18}O_P$ when all data are combined (Figure 2), but the absence of such a correlation when data are subset according to month (Figure 3), is that both T_{max} and $\delta^{18}O_P$ exhibit strong seasonal components which do not affect regressions on sub-monthly timescales. However, although both vary seasonally, a casual relationship between T_{max} and $\delta^{18}O_P$ is not certain and their correlation may instead relate to seasonal changes in a variety of conditions, including moisture source, trajectory, weather type and land surface feedbacks (Baldini et al. 2010; Fischer and Treble 2008; Treble et al. 2005).

Changes in the North Atlantic Oscillation (NAO) (Hurrell 1995) would be expected to influence $\delta^{18}O_P$ as it reflects the position of the westerly jet as a function of air pressure differentials across the North Atlantic, resulting in changes to the source and

trajectory of weather systems and water vapour travelling to the British Isles. However, we observe no significant regression between $\delta^{18}O_P$ and NAO, either when all data are combined or when data are subset according to month (Figures 2c and 3g-i). It should be noted that our data do not comprehensively represent winter (DJF) conditions in the British Isles, the season when NAO is considered to have it's largest effect upon $\delta^{18}O_P$ (Baldini et al. 2008; Fischer and Baldini 2011). Except for January 2012, for which three days sampling is insufficient to examine the role of temporal changes in the NAO, the closest month to winter sampled in this study is March 2010, whereby three sites exhibit significant correlations between NAO and $\delta^{18}O_P$: Horsham, West Moors and Edenbridge (for which March 2010 are the only samples collected) (Figure 6 and Figure S1). Otherwise, none of the other sites, or months examined, exhibit significant effects of the NAO upon British $\delta^{18}O_P$. A generally weak effect of the NAO would contrast with the conclusions of previous studies that the NAO has a significant, positive relationship with winter $\delta^{18}O_P$ (Baldini et al. 2008; Fischer and Baldini 2011). However, the limited coverage of winter rainfall through this study precludes further comment on the effect of NAO upon $\delta^{18}O_P$ and further sampling of daily winter rainfall across a spatial gradient is required to fully address this uncertainty.

The spatial and temporal variability in $P^{0.5}$ and T_{max} coefficients indicates that models derived from individual sites cannot be unilaterally applied, even within relatively small geographical areas such as the British Isles. However, those variable coefficients do provide potential insights into the mechanisms behind the relationship between $\delta^{18}O_P$, $P^{0.5}$ and T_{max}. Rayleigh distillation is a commonly cited simple model for isotope fractionation during water condensation within a cloud (Dansgaard 1964).

As a finite parcel of moisture condenses, Rayleigh fractionation predicts that the initial stages of condensation will be associated with relatively little change in $\delta^{18}O_P$. For example, condensation of the initial 50% of vapour is predicted to equate to an ~ –8‰ decrease in $\delta^{18}O_P$. By contrast, condensation of the final 20% of vapour within a parcel is predicted to impart an isotopic depletion of >30‰ (Dansgaard 1964). The degree of rainout from a vapour parcel is therefore likely to be a simple, first order mechanism which results in an inverse correlation between $\delta^{18}O_P$ and rainfall amount. In reality, a pure Rayleigh distillation is unlikely to occur within a cloud, due to the resupply of moisture from evapotranspiration and mixing between vapour parcels. Furthermore, a wide range of factors introduce complexity, from changes in the isotopic composition of the initial vapour parcel (reflecting the conditions at it's origin and subsequent mixing and phase changes during transit) to the subsequent modification of raindrop $\delta^{18}O$ due to evaporation and equilibrium exchange with ambient vapour (Celle-Jeanton et al. 2004; Gedzelman and Arnold 1994). Nevertheless, some degree of Rayleigh fractionation of atmospheric vapour remains a viable explanation for some of the observed relationships between $\delta^{18}O_P$ and precipitation amount, whereby weather events associated with a high amount of precipitation become progressively isotopically depleted. The rain out effect is non-linear and likely to result in heterogeneous spatial and temporal patterns. In particular, low altitude, coastal sites more frequently encounter vapour parcels in their initial stages of moisture depletion, and consequently precipitation at those locations is less likely to exhibit a marked sensitivity to rainfall amount. By contrast, high altitude and inland sites encounter vapour parcels that have undergone a larger degree of prior rainout, meaning that subsequent condensation and precipitation should exhibit steeper isotope effects. For the maritime climate of the British Isles, this pattern of

progressive rainout may provide one explanation for the spatial and temporal variability in the relationship between $\delta^{18}O_P$ and rainfall amount, whereby $\delta^{18}O_P$ is more sensitive to rainout effects in northern Britain, downstream of the direction of the prevailing weather (Figure 7). By contrast, southern, low elevation sites are less likely to be susceptible to rainout effects and therefore may exhibit correlations with other variables, including temperature and changes in oceanic moisture source. It is important to recognise that due to the temporal migration of weather trajectories, spatial patterns in $\delta^{18}O_P$ and associated correlations with climate variables are unlikely to remain constant in time. A more detailed elucidation of the mechanisms behind isotope fractionation in daily British rainfall could be achieved using isotope enabled climate models, validated or trained against spatially resolved data such as those presented here (Langebroek et al. 2011; Risi et al. 2010). Such an analysis is beyond the scope of this paper but would represent a valuable direction for future research.

Spatial patterns in daily $\delta^{18}O$ relate to weather types

Analysis of $\delta^{18}O_P$ from a highly resolved spatial context provides a means of further deciphering the controls over $\delta^{18}O_P$. This is particularly apparent for the three days in January 2012 for which 70 sites provided $\delta^{18}O_P$ data (Figure 8). On 23rd January 2012, the passage of an occluded front, with low pressure centres to the east and north west of the British Isles resulted in a complex weather pattern (Figure 8b). The majority of atmospheric flow approached the British Isles from the southwest, accounting for the gradient of decreasing $\delta^{18}O_P$ along that trajectory in southern England and Wales (Figure 8a. However, the markedly low $\delta^{18}O_P$ values measured

497 from central Scotland relate to northerly winds travelling along a trough which
498 developed to the north west of Scotland and brought air masses from near Iceland to
499 the British Isles (Figure 8b). On the 24th January, 2012, the previous day's complex
500 weather had passed, and eastern England and Scotland experienced South Westerly
501 weather characterised by a warm front passing perpendicular to the east coast, leading
502 to a characteristic east-west $\delta^{18}O_P$ gradient suggestive of progressive rainout (Figures
503 8d-f). On 25th January 2012, a further cold front arrived in north western Scotland and
504 England and Northern Ireland resulting in moderate isotopic depletion of rainfall in
505 the west, and limited precipitation in the south east (Figures 8g-i).
506
507 The coherency of daily $\delta^{18}O_P$ patterns for the British Isles under different weather-
508 types highlights significant potential for developing an isotope-based synoptic
509 typology, which could then be applied to palaeoclimate research. To do so rigorously
510 would require a much more detailed study, however the data obtained to date
511 highlight some encouraging patterns. The rainfall events sampled through this study
512 predominantly occurred during two common weather types: Cyclonic and South
513 Westerly weather types (according to the Lamb Weather Type scheme). Although it is
514 not possible to make conclusive statements on the way these weather types are
515 manifest in daily $\delta^{18}O_P$ over the British Isles, there is evidence to suggest that the
516 rotational flow associated with Cyclonic weather types is manifest in a progressive
517 south-north $\delta^{18}O_P$ gradient, which curves around a region of maximum isotopic
518 depletion (lowest $\delta^{18}O_P$), representative of the epicentre of the cyclonic vortex (Figure
519 9). The patterns associated with Cyclonic weather types in the British Isles are
520 similar, if smaller, to those related to cyclonic precipitation in the eastern United
521 States, including storm precipitation (Good et al. 2014; Lawrence and Gedzelman

1996). By contrast we are not yet able to make generalisations concerning the spatial $\delta^{18}O_P$ patterns associated with South Westerly weather types, for which the data to date exhibit less coherent patterns in space (Figure 10). These varying isotopic spatial gradients associated with South Westerly weather types may reflect complex or heterogeneous rainfall patterns across the country and associated fractionation processes. Within this context, complexities arise owing to variability in the direction of flow and the interaction between numerous air parcels. For example, our data to date are insufficient to identify and evaluate the effect of frontal rainfall upon $\delta^{18}O_P$, however it is expected that the passage of, and interaction between, warm and cold fronts would cause significant intra- and inter-daily variability in $\delta^{18}O_P$ due to localised changes in air pressure, the altitude of precipitation formation and air temperature (Celle-Jeanton et al. 2004; Celle-Jeanton et al. 2001). Furthermore, a number of weather types are only sporadically captured in our dataset (Figure S5) and future research should therefore attempt to undertake a more detailed and prolonged monitoring project in order to develop a synoptic typology of $\delta^{18}O_P$ for the British Isles.

Conclusion

Daily monitoring of the oxygen isotope composition of rainfall from multiple sites across the British Isles reveals a relationship between rainfall amount (square root transformed; $P^{0.5}$) and $\delta^{18}O_P$, which emerges when all data are combined and when the data are subset according to month or site. By contrast, daily maximum air temperature (T_{max}) exerts a weaker and less consistent relationship and daily NAO exhibits limited influence, although winter conditions are not extensively sampled in

our data. The $P^{0.5}$ and T_{max} regression coefficients and r^2 vary seasonally, in support of previous observations from Dublin, Ireland (Fischer and Baldini 2011). They also vary spatially, with a greater influence of temperature in southern sites, and greater influence of precipitation amount at northern sites. We propose a simple explanation that these spatio-temporal patterns in regression coefficients reflect the non-linear influence of Rayleigh fractionation and rainout upon $\delta^{18}O_P$ as a vapour parcel becomes progressively depleted. Future research involving the integration of climate models with highly resolved data such as ours should be directed at testing this interpretation. By mapping the distribution of daily $\delta^{18}O_P$ across the British Isles, we are able to observe patterns that may be characteristic of some weather types, namely Cyclonic weather types under the Lamb classification scheme. These observations are a step towards an improved mechanistic understanding of the climate controls over $\delta^{18}O_P$ and a synoptic typology which will aid attempts to reconstruct past changes in dominant weather patterns.

Acknowledgements

This research is heavily indebted to the voluntary weather monitors affiliated with the U.K. Met Office and the Climate Observers Link, whose enthusiasm and diligence in collecting daily rainfall samples was central to the conduct of this study – thank you. In particular we thank Sarah Dunn, Ruth Brookshaw, Mike Cinderey, Mike Chalton, John Walker, Jane Corey, David King, Kirsty Murfitt, Richard Griffith, Margaret Airy, Donald Perkins, Malham Tarn FSC Field Centre Staff, Eric Gilbert, Roland Bol, George Darling and Martin Rowley. We thank Joseph Bailey for assistance in producing one of the figures and Bronwyn Dixon for her advice on HYSPLIT

572 modelling. The research was supported by the U.K. Natural Environment Research
573 Council (NERC) through a Fellowship (NE/F014708/1) to JJT. MJ thanks the School
574 of Geography, Planning and Environmental Management at the University of
575 Queensland for a Visiting Fellowship during which some of this manuscript was
576 written. Three anonymous reviewers and the editor Jean Claude Duplessey are
577 thanked for their insightful comments on an earlier draft of this manuscript.
578
579
580

Table 1

Details of sites sampled during March 2010, October 2010 and July 2011. Site numbers relate to those mapped in Figure 1. Values within the 'Sample months' columns indicate the number of samples collected in each month, at each site. Details of nearby Met Office stations used to complement data where no local temperature measurements were taken are given in the 'Notes' column.

					Sample months			
Site	**Site No.**	**Latitude (°N)**	**Longitude (°E)**	**Height (m.a.s.l.)**	**March 2010**	**October 2010**	**July 2011**	**Notes**
Aboyne	1	57.07	-2.79	126		15	11	
Acton	2	53.07	-2.55	44	10		10	Temperature data from MIDAS (site 1132; Reaseheath Hall; 2km NE)
Carlton-in-Cleveland	3	54.43	-1.22	88	11	15	14	
Darvel	4	55.60	-4.23	217	10	14	15	
Eastry	5	51.25	1.31	32	10	15	11	
Ebbw Vale	6	51.74	-3.18	303	10	15	14	
Edenbridge	7	51.20	0.07	47	10			
Glenmore Lodge	8	57.17	-3.68	344		13	17	Temperature data from MIDAS (site 118; Cairngorm Chairlift; 4km S)
Horsham	9	51.07	-0.34	37	10	13	8	
Lawkland	10	54.09	-2.34	176	10			Temperature data from MIDAS (site 513; Bingley; 44km SW)
Llansadwrn	11	53.26	-4.17	107	11	19	15	
Lunan Vale	12	56.66	-2.51	19		15	15	Temperature data from MIDAS (site 15045; Crombie Country Park; 19km SW)
Malham Tarn	13	54.10	-2.16	384		15	13	
Marlborough	14	51.43	-1.73	142	10	15	2	
Okehampton	15	50.74	-4.00	170		15	14	Temperature data from MIDAS (site 1345; East Okement Farm; 4km S)
Wallingford	16	51.60	-1.11	50		10	9	
West Moors	17	50.82	-1.88	17	10	13	12	
Total samples					**102**	**202**	**180**	

587
588

589 **Figure Captions**

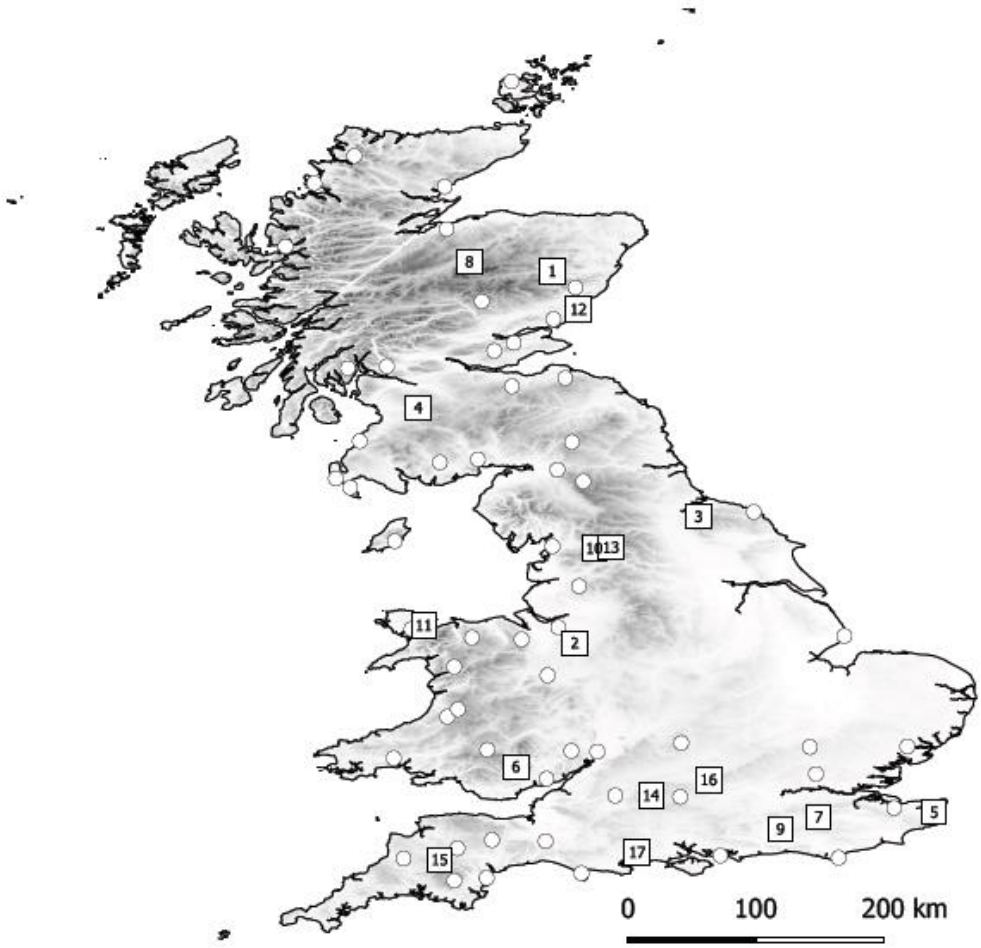

590

591 **Fig. 1**

592 Topographic map of the British Isles (dark shaded areas = higher elevation), including
593 the location of the sampling sites used in this study. Open circles are those sites only
594 sampled in January 2012, whereas open boxes indicate the sites sampled during all
595 months. The numbers in the squares indicates the site number, as detailed in Table 1.

596

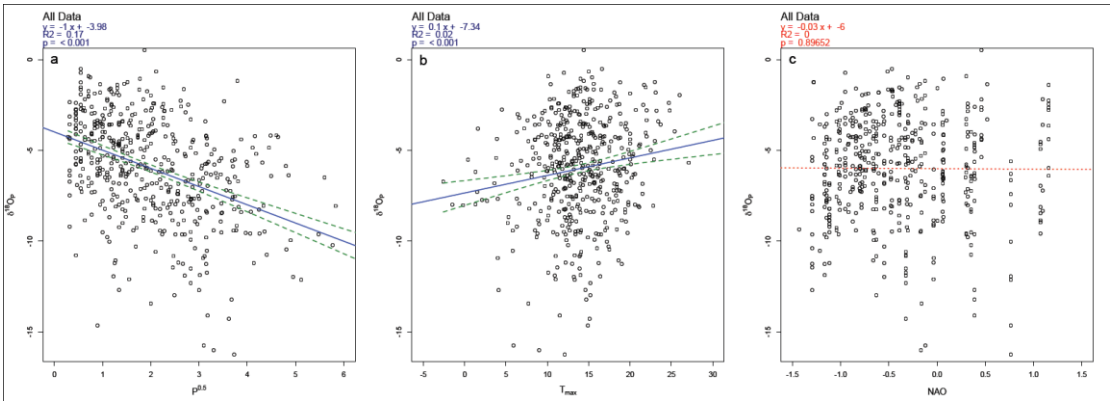

Fig. 2

Scatter plots of daily $\delta^{18}O_P$ vs. (a) precipitation amount (square root transformed; $P^{0.5}$), (b) daily maximum temperature (T_{max}) and (c) North Atlantic Oscillation index (NAO) for all samples collected during March 2010, October 2010 and July 2011. Regression coefficients are given inset. Solid blue lines = significant linear model fit, dashed green lines = 95% confidence intervals. Non-significant linear models are illustrated with dotted red lines. Blue text relates to significant regression models, whereas red text indicates non-significant models.

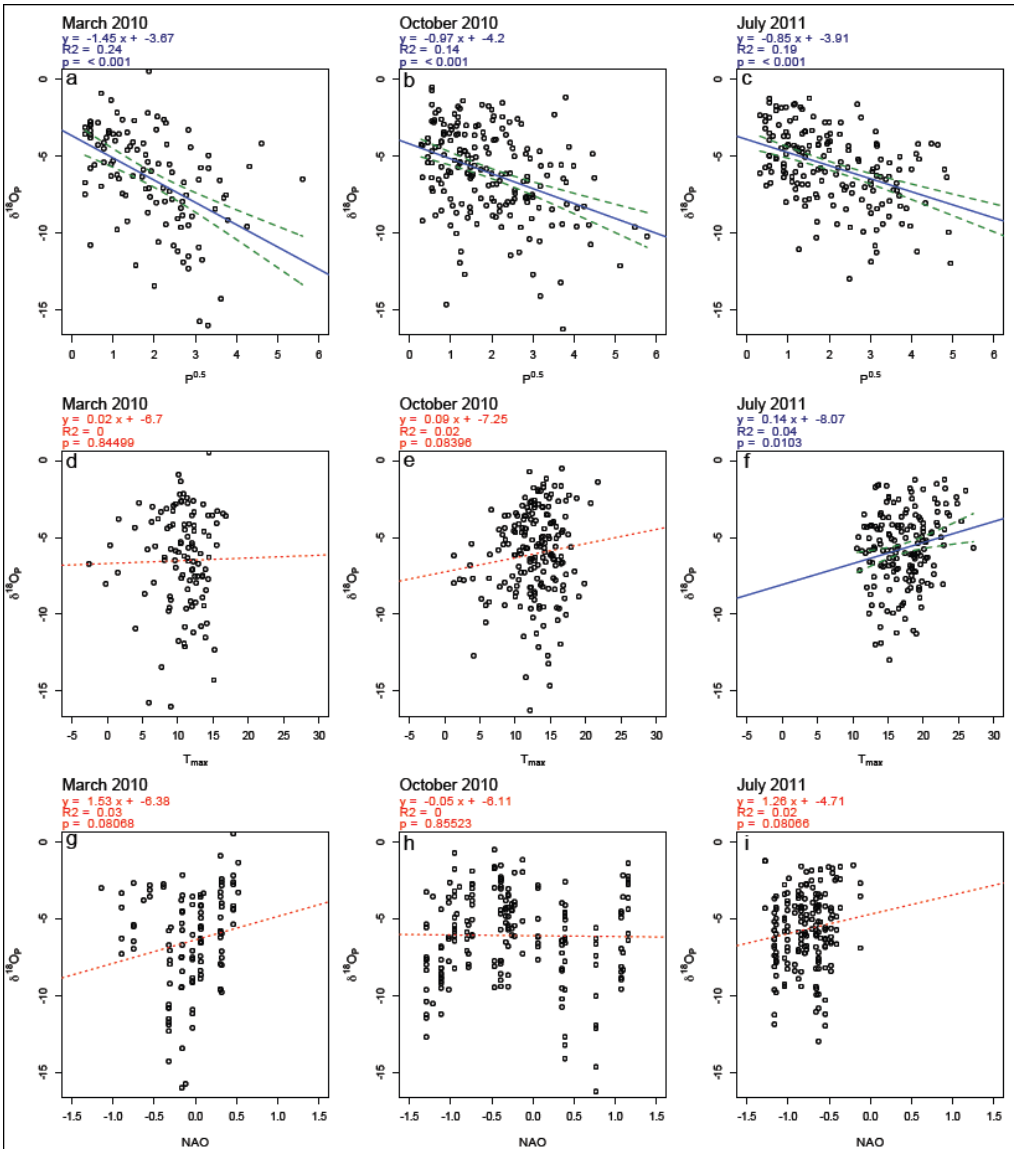

Fig. 3

Scatter plots of daily $\delta^{18}O_P$ vs. (a, d, g) precipitation amount (square root transformed, $P^{0.5}$), (b, e, h) daily maximum temperature (T_{max}) and (c, f, i) North Atlantic Oscillation index (NAO) for all samples subset according to month of sampling collected during March 2010, October 2010 and July 2011. Regression coefficients are given inset. Solid blue lines = linear model fit and dashed green lines = 95% confidence intervals for significant regressions. Non-significant linear models are illustrated with dotted red lines. Blue text relates to significant regression models, whereas red text indicates non-significant models.

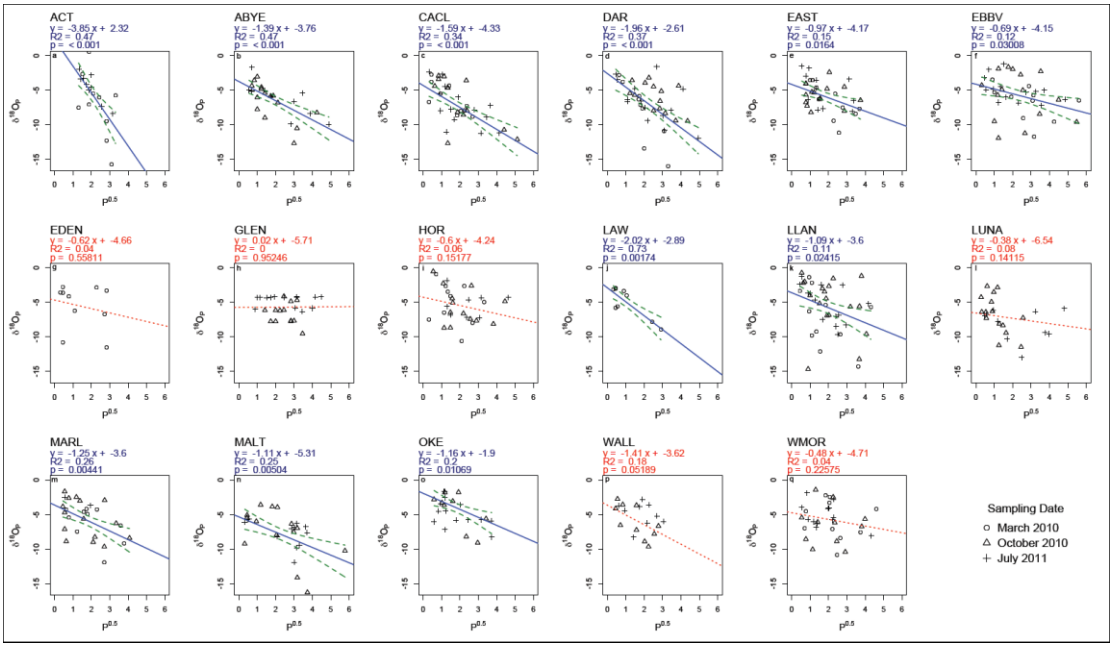

Fig. 4

Scatter plots of daily $\delta^{18}O_P$ vs precipitation amount (square root transformed, $P^{0.5}$) subset by site for all samples collected during March 2010 (open circles), October 2010 (open triangles) and July 2011 (crosses). Regression coefficients are given inset. Solid blue lines = linear model fit and dashed green lines = 95% confidence intervals for significant regressions. Non-significant linear models are illustrated with dotted red lines. Blue text relates to significant regression models, whereas red text indicates non-significant models.

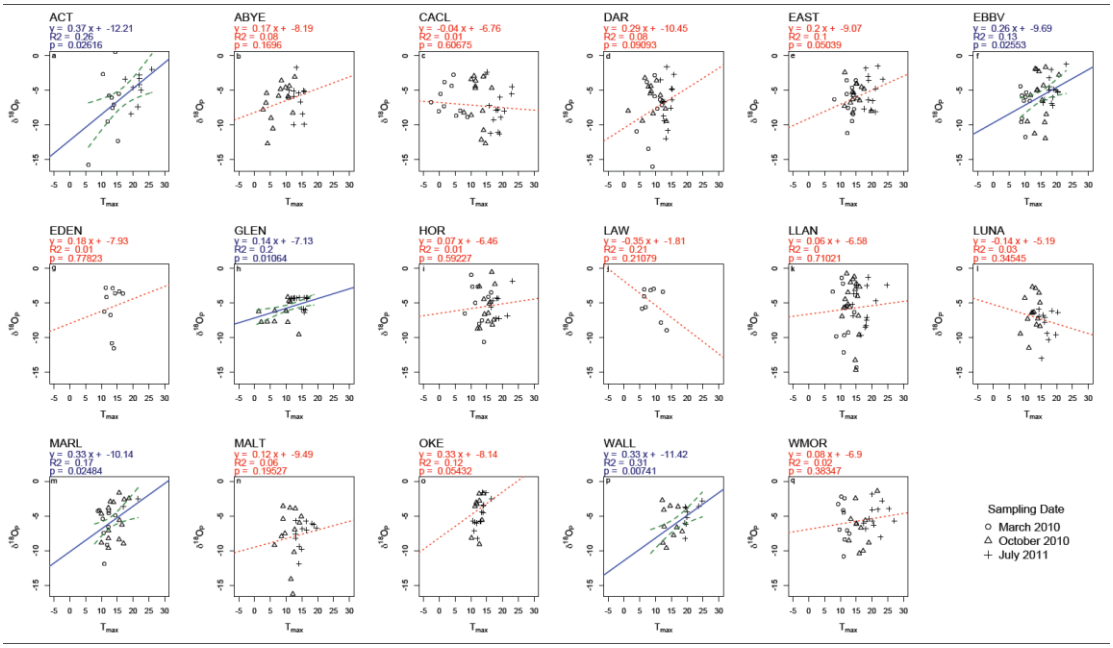

627

628 **Fig. 5**

629 Scatter plots of daily $\delta^{18}O_P$ vs. daily maximum temperature (T_{max}) subset by site for
630 all samples collected during March 2010 (open circles), October 2010 (open triangles)
631 and July 2011 (crosses). Regression coefficients are given inset. Solid blue lines =
632 linear model fit and dashed green lines = 95% confidence intervals for significant
633 regressions. Non-significant linear models are illustrated with dotted red lines. Blue
634 text relates to significant regression models, whereas red text indicates non-significant
635 models.

636

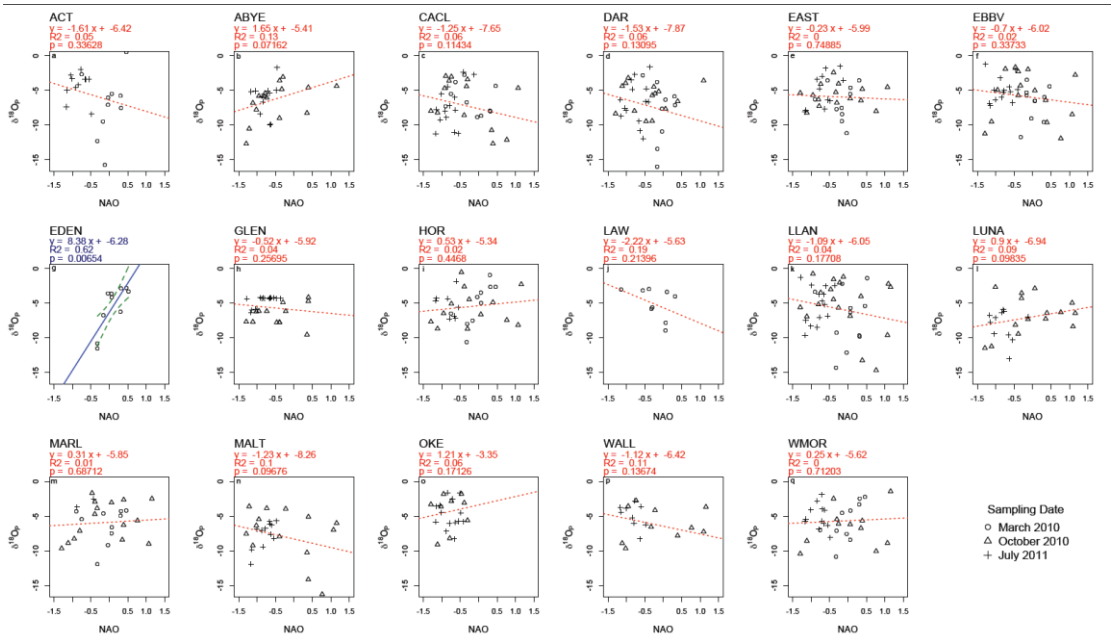

Fig. 6

Scatter plots of daily $\delta^{18}O_P$ vs. North Atlantic Oscillation index (NAO) subset by site for all samples collected during March 2010 (open circles), October 2010 (open triangles) and July 2011 (crosses). Regression coefficients are given inset. Solid blue lines = linear model fit and dashed green lines = 95% confidence intervals for significant regressions. Non-significant linear models are illustrated with dotted red lines. Blue text relates to significant regression models, whereas red text indicates non-significant models.

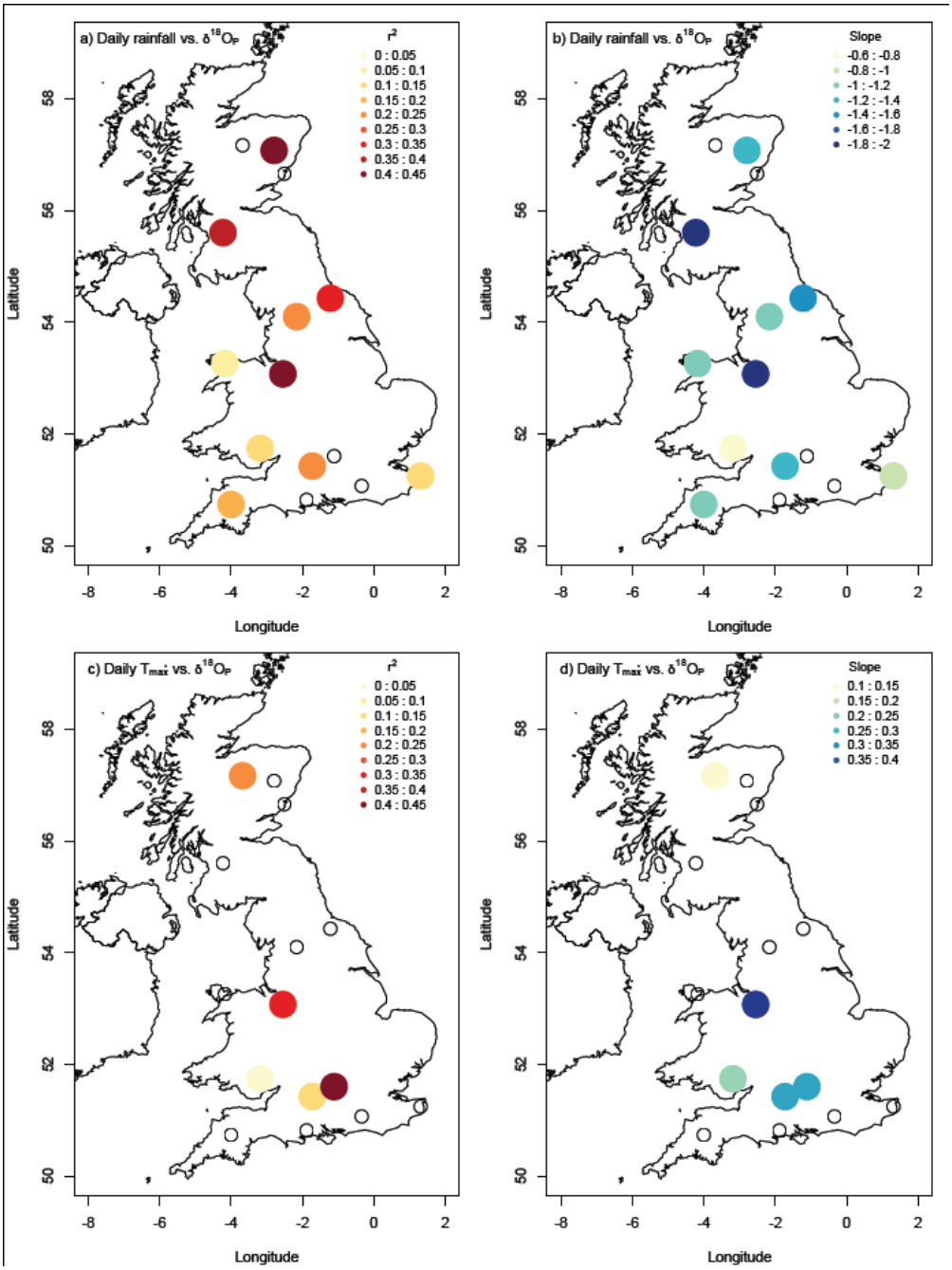

Fig. 7

Map of regression coefficients against daily rainfall amount (square root transformed, $P^{0.5}$) and daily maximum temperature (T_{max}) for all sites in Table 1, except Edenbridge and Lawkland, for which only one month's data were collected. (a) r^2 statistic for $P^{0.5}$ vs. $\delta^{18}O_P$; (b) slope for $P^{0.5}$ vs. $\delta^{18}O_P$; (c) r^2 statistic for T_{max} vs. $\delta^{18}O_P$; (d) slope for T_{max} vs. $\delta^{18}O_P$. Open circles indicate the location of sites for which no significant regression was observed for the variable mapped.

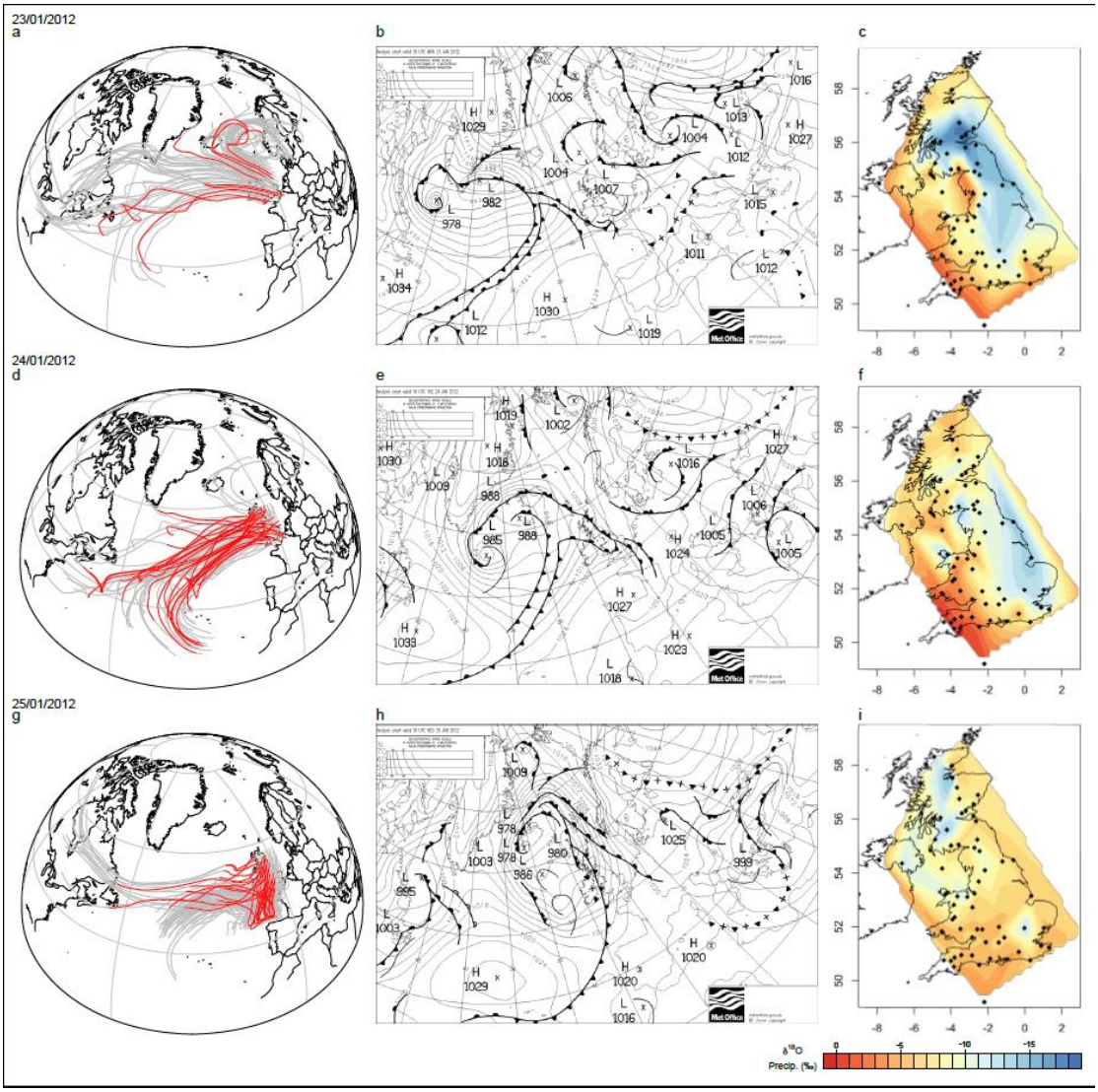

Fig. 8

Weather and isotope maps for 23rd, 24th and 25th January 2012. (a, d, g) HYSPLIT 96 hour back trajectories for air parcels arriving at a matrix of 63 points across the British Isles. All simulations start at 1500 m.a.s.l. Grey lines indicate all back trajectories, red lines are those whereby significant moisture uptake is estimated. The length of the red lines indicates the distance from the initial site of moisture uptake. (b, e, h) Daily weather maps, as reported by the U.K. Met Office. (c, f, i) The spatial distribution of $\delta^{18}O_P$ based on upto 70 monitoring stations, collecting precipitation water at 9 am the following day.

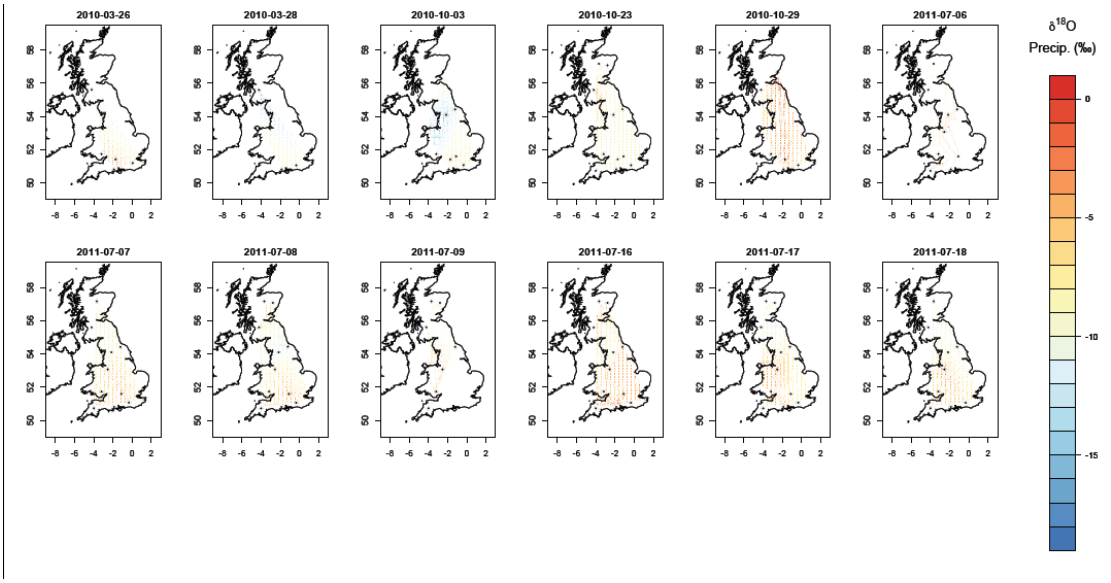

666

667 **Fig. 9**

668 Spatial pattern of $\delta^{18}O_P$ occurring on days with a Cyclonic weather pattern (Lamb

669 Weather Type = 20)

670

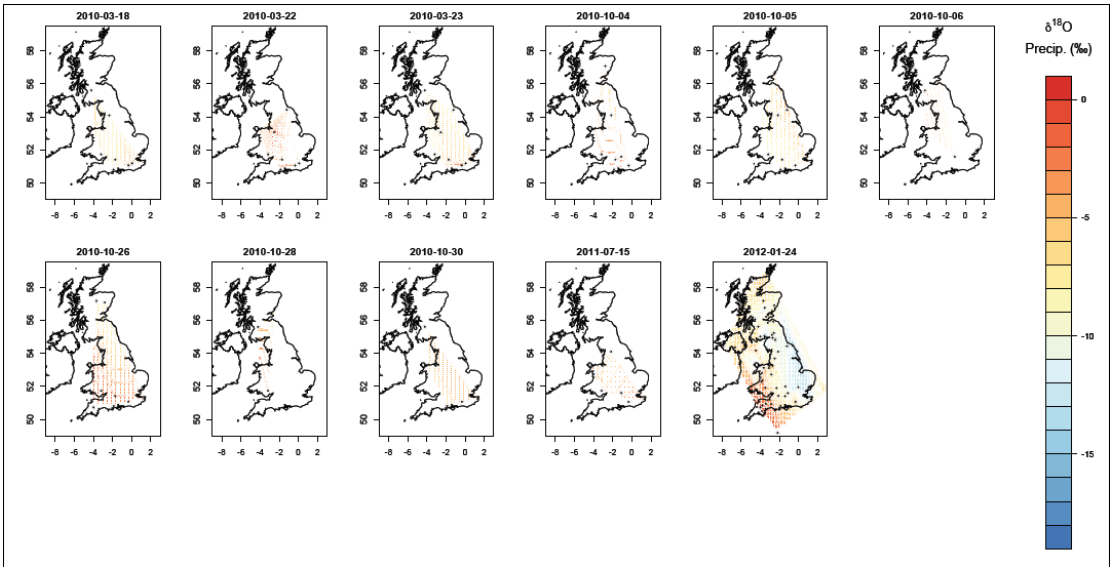

671

672 **Fig. 10**

673

674 Spatial pattern of $\delta^{18}O_P$ occurring on days with a South Westerly weather pattern

675 (Lamb Weather Type = 15)

676

677 **References**

678

679 Akima H (1978) A method of bivariate interpolation and smooth surface fitting for
680 irregularly distributed data points ACM Transactions on Mathematical
681 Software 4:148-159 doi:10.1145/355780.355786

682 Araguas-Araguas L, Froehlich K, Rozanski K (2000) Deuterium and oxygen-18
683 isotope composition of precipitation and atmospheric moisture Hydrological
684 Processes 14:1341-1355

685 Baker A et al. (2011) High resolution delta O-18 and delta C-13 records from an
686 annually laminated Scottish stalagmite and relationship with last millennium
687 climate Global and Planetary Change 79:303-311
688 doi:10.1016/j.gloplacha.2010.12.007

689 Baldini LM, McDermott F, Baldini JUL, Fischer MJ, Moellhoff M (2010) An
690 investigation of the controls on Irish precipitation d18O values on monthly
691 and event timescales Climate Dynamics 35:977-993

692 Baldini LM, McDermott F, Foley AM, Baldini JUL (2008) Spatial variability in the
693 European winter precipitation delta(18)O-NAO relationship: Implications for
694 reconstructing NAO-mode climate variability in the Holocene Geophysical
695 Research Letters 35 doi:10.1029/2007gl032027

696 Barbante C et al. (2006) One-to-one coupling of glacial climate variability in
697 Greenland and Antarctica Nature 444:195-198 doi:10.1038/nature05301

698 Bowen GJ, Wilkinson B (2002) Spatial distribution of delta O-18 in meteoric
699 precipitation Geology 30:315-318

700 Callow N, McGowan H, Warren L, Speirs J (2014) Drivers of precipitation stable
701 oxygen isotope variability in an alpine setting, Snowy Mountains, Australia
702 Journal of Geophysical Research-Atmospheres 119:3016-3031
703 doi:10.1002/2013jd020710

704 Celle-Jeanton H, Gonfiantini R, Travi Y, Sol B (2004) Oxygen-18 variations of
705 rainwater during precipitation: application of the Rayleigh model to selected
706 rainfalls in Southern France Journal of Hydrology 289:165-177

707 Celle-Jeanton H, Travi Y, Blavoux B (2001) Isotopic typology of the precipitation in
708 the Western Mediterranean region at three different time scales Geophysical
709 Research Letters 28:1215-1218

710 Crawford J, Hughes CE, Parkes SD (2013) Is the isotopic composition of event based
711 precipitation driven by moisture source or synoptic scale weather in the

712 Sydney Basin, Australia? Journal of Hydrology 507:213-226
713 doi:10.1016/j.jhydrol.2013.10.031

714 Dansgaard W (1964) Stable Isotopes in Precipitation Tellus 16:436-468

715 Dansgaard W et al. (1993) Evidence for General Instability of Past Climate from A
716 250-Kyr Ice-Core Record Nature 364:218-220

717 Darling WG, Talbot JC (2003) The O & H stable isotopic composition of fresh waters
718 in the British Isles. 1. Rainfall Hydrology and Earth System Sciences 7:163-
719 181

720 Draxler RR, Hess GD (1997) Description of the HYSPLIT_4 modeling system. .
721 NOAA Technical Memo. ERL ARL-244. NOAA Air Resources Laboratory,
722 Silver Spring MD

723 Draxler RR, Hess GD (1998) An overview of the HYSPLIT_4 modelling system for
724 trajectories, dispersion and deposition Australian Meteorological Magazine
725 47:295-308

726 Draxler RR, Rolph GD (2015) HYSPLIT (HYbrid Single-Particle Lagrangian
727 Integrated Trajectory) NOAA Air Resources Laboratory, Silver Spring, MD

728 Evans MN, Schrag DP (2004) A stable isotope-based approach to tropical
729 dendroclimatology Geochimica Et Cosmochimica Acta 68:3295-3305
730 doi:10.1016/j.gca.2004.01.006

731 Fischer MJ, Baldini L (2011) A climate-isotope regression model with seasonally-
732 varying and time-integrated relationships Climate Dynamics doi:DOI:
733 10.1007/s00382-011-1009-1

734 Fischer MJ, Treble PC (2008) Calibrating climate-delta O-18 regression models for
735 the interpretation of high-resolution speleothem delta O-18 time series Journal
736 of Geophysical Research-Atmospheres 113 doi:10.1029/2007jd009694

737 Gedzelman SD, Arnold R (1994) Modeling the Isotopic Composition of Precipitation
738 Journal of Geophysical Research-Atmospheres 99:10455-10471

739 Good SP, Mallia DV, Lin JC, Bowen GJ (2014) Stable Isotope Analysis of
740 Precipitation Samples Obtained via Crowdsourcing Reveals the
741 Spatiotemporal Evolution of Superstorm Sandy Plos One 9
742 doi:10.1371/journal.pone.0091117

743 Heathcote JA, Lloyd JW (1986) Factors Affecting the Isotopic Composition of Daily
744 Rainfall at Driby, Lincolnshire Journal of Climatology 6:97-106

745 Hoffmann G, Cuntz M, Werner M, Jouzel J, Aggarwal PK, Gat JR, Froehlich K
746 (2006) A systematic comparison between the IAEA/GNIP isotope network
747 and Atmospheric General Circulation Models: How much climate information
748 is in the water isotopes? In: Isotopes in the Water Cycle - Past, Present and
749 Future of a Developing Science. Springer, Berlin, pp 303-320

750 Hurrell JW (1995) Decadal Trends in the North-Atlantic Oscillation - Regional
751 Temperatures and Precipitation Science 269:676-679

752 Johnsen SJ et al. (2001) Oxygen isotope and palaeotemperature records from six
753 Greenland ice-core stations: Camp Century, Dye-3, GRIP, GISP2, Renland
754 and NorthGRIP Journal of Quaternary Science 16:299-307

755 Jones MD, Leng MJ, Arrowsmith C, Deuchar C, Hodgson J, Dawson T (2007) Local
756 d18O and d2H variability in UK rainfall. Hydrology and Earth System Science
757 Discussions 4

758 Jones MD, Roberts CN, Leng MJ, Turkes M (2006) A high-resolution late Holocene
759 lake isotope record from Turkey and links to North Atlantic and monsoon
760 climate Geology 34:361-364

761 Jones PD, Hulme M, Briffa KR (1993) A Comparison of Lamb Circulation Types
762 with An Objective Classification Scheme International Journal of Climatology
763 13:655-663

764 Jouzel J, Hoffmann G, Koster RD, Masson V (2000) Water isotopes in precipitation:
765 data/model comparison for present-day and past climates Quat Sci Rev
766 19:363-379

767 Kohn MJ, Welker JM (2005) On the temperature correlation of delta O-18 in modem
768 precipitation Earth and Planetary Science Letters 231:87-96
769 doi:10.1016/j.epsl.2004.12.004

770 Krklec K, Dominguez-Villar D (2014) Quantification of the impact of moisture
771 source regions on the oxygen isotope composition of precipitation over Eagle
772 Cave, central Spain Geochimica Et Cosmochimica Acta 134:39-54
773 doi:10.1016/j.gca.2014.03.011

774 Lachniet MS, Patterson WP (2009) Oxygen isotope values of precipitation and
775 surface waters in northern Central America (Belize and Guatemala) are
776 dominated by temperature and amount effects Earth and Planetary Science
777 Letters 284:435-446 doi:10.1016/j.epsl.2009.05.010

778 Lamb HH (1950) Types and spells of weather around the year in the British Isles -
779 annual trends, seasonal structure of the year, singularities Quarterly Journal of
780 the Royal Meteorological Society 76:393-438 doi:10.1002/qj.49707633005

781 Langebroek PM, Werner M, Lohmann G (2011) Climate information imprinted in
782 oxygen-isotopic composition of precipitation in Europe Earth and Planetary
783 Science Letters 311:144-154

784 Lawrence JR, Gedzelman SD (1996) Low stable isotope ratios of tropical cyclone
785 rains Geophysical Research Letters 23:527-530

786 Liebminger A, Haberhauer G, Papesch W, Heiss G (2006) Correlation of the isotopic
787 composition in precipitation with local conditions in alpine regions Journal of
788 Geophysical Research-Atmospheres 111

789 Merlivat L (1978) Molecular diffusivities of (H2O)-O-16, HD16O and (H2O)-O-18 in
790 gases Journal of Chemical Physics 69:2864-2871 doi:10.1063/1.436884

791 Merlivat L, Jouzel J (1979) Global Climatic Interpretation of the Deuterium-Oxygen-
792 18 Relationship for Precipitation Journal of Geophysical Research-Oceans and
793 Atmospheres 84:5029-5033

794 Merlivat L, Nief G (1967) Fractionment isotopique lors des changements detat solide-
795 vapeur et liquide-vapeur de leau a des temperatures inferieures a 0 degrees C
796 Tellus 19:122-127

797 PAGES 2k Consortium (2013) Continental-scale temperature variability during the
798 past two millennia Nature Geoscience 6:339-346

799 Petit JR et al. (1999) Climate and atmospheric history of the past 420,000 years from
800 the Vostok ice core, Antarctica Nature 399:429-436

801 Risi C, Bony S, Vimeux F, Jouzel J (2010) Water-stable isotopes in the LMDZ4
802 general circulation model: Model evaluation for present-day and past climates
803 and applications to climatic interpretations of tropical isotopic records Journal
804 of Geophysical Research 115:D24123

805 Robertson I, Waterhouse JS, Barker AC, Carter AHC, Switsur VR (2001) Oxygen
806 isotope ratios of oak in east England: implications for reconstructing the
807 isotopic composition of precipitation Earth and Planetary Science Letters
808 191:21-31

809 Rolph GD (2015) Real-time Environmental Applications and Display sYstem
810 (READY). NOAA Air Resources Laboratory, Silver Springs, MD

811 Rozanski K, Araguas-Araguas L, Gonfiantini R, Swart PK, Lohman KC, McKenzie J,
812 Savin SM (1993) Isotopic patterns in modern global precipitation. In: Climate
813 change in continental isotopic records, vol 78. Geophysical Monograph.
814 American Geophysical Union, pp 1-36

Rozanski K, Araguasaraguas L, Gonfiantini R (1992) Relation Between Long-Term Trends of O-18 Isotope Composition of Precipitation and Climate Science 258:981-985

Schmidt GA, LeGrande AN, Hoffmann G (2007) Water isotope expressions of intrinsic and forced variability in a coupled ocean-atmosphere model Journal of Geophysical Research-Part D-Atmospheres 112:1-18 doi:10.1029/2006jd007781

Shakun JD, Carlson AE (2010) A global perspective on Last Glacial Maximum to Holocene climate change Quat Sci Rev 29:1801-1816

Sodemann H, Masson-Delmotte V, Schwierz C, Vinther BM, Wernli H (2008) Interannual variability of Greenland winter precipitation sources: 2. Effects of North Atlantic Oscillation variability on stable isotopes in precipitation Journal of Geophysical Research-Atmospheres 113 doi:10.1029/2007jd009416

Treble PC, Budd WF, Hope PK, Rustomji PK (2005) Synoptic-scale climate patterns associated with rainfall delta O-18 in southern Australia Journal of Hydrology 302:270-282

Tyler JJ, Leng MJ, Sloane HJ, Sachse D, Gleixner G (2008) Oxygen isotope ratios of sedimentary biogenic silica reflect the European transcontinental climate gradient Journal of Quaternary Science 23:341-350

Vachon RW, White JWC, Gutmann E, Welker JM (2007) Amount-weighted annual isotopic (delta O-18) values are affected by the seasonality of precipitation: A sensitivity study Geophysical Research Letters 34 doi:10.1029/2007gl030547

von Grafenstein U, Erlenkeuser H, Muller J, Trimborn P, Alefs J (1996) A 200 year mid-European air temperature record preserved in lake sediments: An extension of the delta O-18(P)-air temperature relation into the past Geochimica et Cosmochimica Acta 60:4025-4036

Wang YJ et al. (2008) Millennial- and orbital-scale changes in the East Asian monsoon over the past 224,000 years Nature 451:1090-1093 doi:10.1038/nature06692